JOURNAL OF CATALYSIS **178,** 153–173 (1998)
ARTICLE NO. CA982134

In Situ Infrared Study of Methanol Synthesis from H_2/CO over Cu/SiO_2 and $Cu/ZrO_2/SiO_2$

Ian A. Fisher and Alexis T. Bell[1]

Chemical Sciences Division, Lawrence Berkeley National Laboratory, and Department of Chemical Engineering, University of California, Berkeley, California 94720-1462

Received November 11, 1997; revised March 27, 1998; accepted April 28, 1998

The interactions of CO and H_2/CO with Cu/SiO_2, ZrO_2/SiO_2, and $Cu/ZrO_2/SiO_2$ have been investigated by in situ infrared spectroscopy with the aim of understanding the nature of the species involved in methanol synthesis and the dynamics of the formation and consumption of these species. In the case of Cu/SiO_2, carbonate species adsorbed on Cu and methoxide species adsorbed on Cu and silica are observed at 523 K, $H_2/CO = 3$, and a total pressure of 0.65 MPa. When ZrO_2/SiO_2 or $Cu/ZrO_2/SiO_2$ is exposed to H_2/CO, the majority of the species observed are associated with ZrO_2. CO adsorption on either ZrO_2/SiO_2 or $Cu/ZrO_2/SiO_2$ results in the formation of carboxylate, bicarbonate, and formate species on zirconia. In the presence of H_2, formate species are hydrogenated to methoxide species adsorbed on ZrO_2. The presence of Cu greatly accelerates the rate of formate hydrogenation to methoxide species, a process in which methylenebisoxy species are observed as intermediates. Cu also significantly promotes the reductive elimination of methoxide species as methanol. Thus, methanol synthesis over $Cu/ZrO_2/SiO_2$ is envisioned to occur on ZrO_2, with the primary role of Cu being the dissociative adsorption of H_2. The spillover of atomic H onto ZrO_2 provides the source of hydrogen needed to hydrogenate the carbon-containing species. Spillover of absorbed CO from Cu to zirconia facilitates formate formation on zirconia at lower temperatures than in the absence of Cu. The reductive elimination of methoxide species appears to be the slow step in methanol formation by CO hydrogenation. The lower rate of methanol synthesis over $Cu/ZrO_2/SiO_2$ from CO as compared to CO_2 hydrogenation is attributed to the lack of water formation in the former reaction, preventing facile release of methoxide by hydrolysis. The enhanced rate of methanol synthesis from CO over $Cu/ZrO_2/SiO_2$ as compared to Cu/SiO_2 is attributed to the lower energy-barrier (formate) pathway available on $Cu/ZrO_2/SiO_2$.

INTRODUCTION

Studies of methanol synthesis over supported Cu catalysts have shown that the catalytic activity of Cu is influenced by the choice of support (1–3). Of the various supports investigated, zirconia is particularly interesting because it enhances the activity of Cu for both CO and CO_2 hydrogenation (2, 4–14). In situ investigations of the species formed on Cu- and zirconia-containing catalysts have served as a basis for suggesting the nature of the intermediates involved in the formation of methanol and the pathway by which methanol is formed. Baiker and coworkers (15–17) have reported that for both CO and CO_2 hydrogenation, the reduction of adsorbed CO results in methanol formation via formaldehyde and methoxide intermediates on Cu/ZrO_2. In the case of CO_2 hydrogenation, adsorbed CO is formed by the reduction of surface carbonate, which is formed by CO_2 adsorption. Previous work by the present authors (18) suggests that during CO_2 hydrogenation over Cu/ZrO_2 and $Cu/ZrO_2/SiO_2$, CO_2 adsorbs on the zirconia to form bicarbonate species, which then undergo hydrogenation to produce formate, methylenebisoxy, and finally methoxide species. The hydrogen required for the progressive hydrogenation of the zirconia-bound carbonaceous species is provided by spillover of dissociatively adsorbed H_2 on Cu. Water, the principal by-product of methanol synthesis from CO_2, hydrolyzes the methoxide species adsorbed on zirconia, thereby releasing methanol and restoring zirconia hydroxyl groups required for CO_2 adsorption as bicarbonate. It is also suggested that the reverse-water-gas-shift (RWGS) reaction occurs predominantly on the surface of Cu and is not affected significantly by the presence of zirconia.

In the present study, the interactions of CO and H_2/CO with Cu/SiO_2, ZrO_2/SiO_2, and $Cu/ZrO_2/SiO_2$ catalysts were investigated at 0.65 MPa by in situ FTIR spectroscopy. This work was undertaken to provide further insight into the nature of the surface species present under reaction conditions and their relationship to the mechanism of methanol synthesis. It was of particular interest to determine whether the concept of Cu-promoted synthesis of methanol over zirconia, established in our studies of methanol synthesis from CO_2/H_2 over $Cu/ZrO_2/SiO_2$, would also hold for methanol synthesis from CO/H_2. A further aim of the present work was to identify the reasons for differences in the rates of methanol synthesis from CO and CO_2 observed under comparable conditions (14).

[1] To whom correspondence should be addressed.

0021-9517/98 $25.00

EXPERIMENTAL

The preparation and characterization of the Cu/SiO_2 and $Cu/ZrO_2/SiO_2$ catalysts used in this study have been described elsewhere (14). ZrO_2 was dispersed on SiO_2 in the same manner used to disperse ZrO_2 on Cu/SiO_2 (14). The Cu and Zr contents of the catalysts were determined by X ray fluorescence analysis. The Cu surface areas of the catalysts were determined by N_2O titration (14). By these methods, the Cu/SiO_2 catalyst was determined to contain 5.7 wt% Cu with a Cu surface area of 1.36 m^2/g of catalyst (3.7% Cu dispersion); the ZrO_2/SiO_2 catalyst contained 32.6 wt% ZrO_2; and the $Cu/ZrO_2/SiO_2$ catalyst contained 5.7 wt% Cu with a Cu surface area of 0.76 m^2/g of catalyst (2.1% Cu dispersion), and 30.5 wt% ZrO_2.

Matheson UHP CO, H_2, and He were purified prior to use. CO was passed through a bed of glass beads maintained at 573 K to decompose iron carbonyls, followed by passage through an ascarite trap to remove CO_2 and a molecular sieve trap (3A Davison grade 564) to remove water. Hydrogen was passed through a Deoxo unit (Engelhard) to remove O_2 impurities by forming water, which was subsequently removed by a molecular sieve trap. He was passed through an oxysorb (CrO_2) trap to remove O_2 and then a molecular sieve trap. Purified gases were delivered to the infrared cell via Tylan Model FC-280 mass flow controllers.

In situ transmission infrared spectroscopy was performed using 2-cm diameter catalyst disks of 0.2 mm thickness, weighing approximately 75 mg. The catalyst disks were contained in a low dead volume infrared cell (19). Infrared spectra were collected using a Nicolet Magna 750 series II FTIR spectrometer. Signals were obtained from a narrowband MCT detector. In situ absorbance spectra were obtained by collecting 64 scans at 4 cm^{-1} resolution. Each spectrum was then referenced to a spectrum of the catalyst collected at the same temperature under He or H_2 flow, as appropriate. The cell was heated by electrical resistance heaters, and the cell temperature was controlled by an Omega Series CN-2010 programmable temperature controller.

The methanol synthesis activity was determined by placing 150 mg of catalyst into a microreactor connected to a gas manifold and operated at 0.65 MPa with a feed stream containing a 3/1 mixture of H_2 and CO. Product analysis was by mass spectrometry. A more complete description of the apparatus is given in Refs. 14 and 20.

Prior to each experiment with a fresh sample, the catalyst was reduced in 10% H_2/He flowing at 60 cm^3/min and a total pressure of 0.65 MPa. The reduction temperature was raised at 2 K/min from ambient to 523 K, after which the catalyst was further reduced at 523 K for >8 h in pure H_2 flowing at 40 cm^3/min and a pressure of 0.65 MPa. Subsequent reductions were all performed at 523 K in H_2 at 0.65 MPa, but varied in time (always >8 h), to ensure that observable surface species were removed.

RESULTS

The activity of Cu/SiO_2 and $Cu/ZrO_2/SiO_2$ is reported in Table 1. Under the conditions shown in Table 1, it is evident that zirconia addition increases the methanol synthesis activity of the catalyst 59-fold, when activity is expressed on a per gram basis, and 120-fold, when activity is expressed as a turnover frequency based on the number of Cu sites measured by N_2O titration.

Cu/SiO_2

CO adsorption. Figure 1 shows spectra obtained after CO adsorption on Cu/SiO_2 at temperatures between 323 and 523 K. The catalyst was exposed to He/CO at a ratio of 3/1 and a total pressure of 0.65 MPa for 90 min at each temperature. Spectra were taken after subsequent purging in He for 30 min. The only features observed are in the C–O stretching region. The peak at 2105 cm^{-1}, which decreases in intensity and shifts to higher wavenumbers as the temperature is increased, is assigned to CO adsorbed linearly on high-index planes of metallic Cu (2105 cm^{-1}) at low temperature, and CO adsorbed on Cu^{+1} (2120 cm^{-1}) at high temperature (21).

CO hydrogenation. Spectra were obtained while flowing H_2/CO at a ratio of 3 : 1 and a pressure of 0.65 MPa between 323 and 523 K, and were collected after 2 h at each temperature. The feature at 2105–2120 cm^{-1} observed during CO adsorption is obscured by the intense bands caused by gas phase CO. Only during reaction at 523 K were bands observed in the infrared spectra. The appearance of these features and their interpretation is discussed later.

Temporal resolution of surface species. Transient spectra were obtained after switching the feed from H_2 to 3/1 H_2/CO at a total pressure of 0.65 MPa while maintaining the temperature of the Cu/SiO_2 catalyst at 523 K. The results are shown in Fig. 2. In the C–H stretching region, sev-

TABLE 1

Comparison of Methanol Synthesis Activity[a]

	Catalyst	
	Cu/SiO_2	$Cu/ZrO_2/SiO_2$
Mass Specific Rate (moles/s/g-cat)	6.4×10^{-9}	3.8×10^{-7}
Turnover Frequency (1/s)	1.7×10^{-4}	2.1×10^{-2}

[a] Reaction Conditions: T = 523 K, P = 0.65 MPa, H_2/CO = 3/1, catalyst mass = 0.15 g.

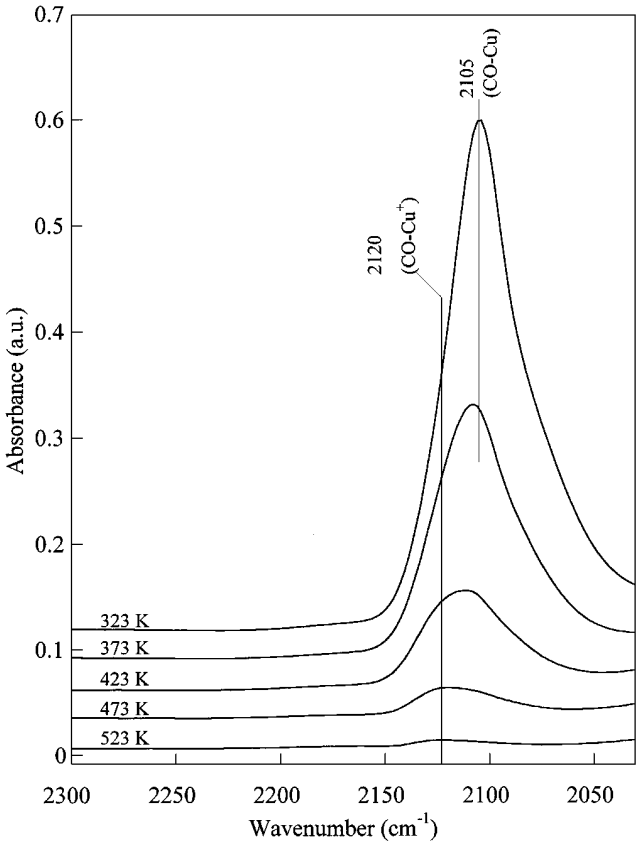

FIG. 1. Infrared spectra taken after purging for 30 min in He following exposure of Cu/SiO_2 to 0.16 MPa CO and 0.49 MPa He flowing at a total rate of 60 cm^3/min. Spectra referenced to Cu/SiO_2 under 0.65 MPa He flow at each temperature.

eral features become apparent at about 2 h and increase in intensity during the remainder of the transient. Bands at 3000(sh), 2962, and 2861 cm^{-1} are assignable to methoxide species on SiO_2 (CH_3O–Si) (18, 22–25). The bands at 2939, 2876 and 2833 cm^{-1}(wk) are assignable to methoxide on Cu (CH_3O–Cu) (23, 24). At lower wavenumbers (1700–1350 cm^{-1}), features become evident after 15 h and increase in intensity during the remainder of the transient. The band at 1464 cm^{-1} is ascribed to CH_3 deformation modes of CH_3O–Si (22, 25), the band at 1454 cm^{-1} is ascribed to CH_3 bending vibrations of CH_3O–Cu (23). The bands at 1415 and 1385 cm^{-1} are assigned to polydentate carbonate on Cu (*p*-CO_3–Cu) (26), the band at 1370 cm^{-1} to monodentate carbonate on Cu (*m*-CO_3–Cu) (18, 27), and the weak peak at 1350 cm^{-1} to bidentate formate on Cu (*b*-HCOO–Cu) (18, 28). The bands at 1485 and 1377 cm^{-1} are similar to bands observed during methanol adsorption on Cu/SiO_2 above 373 K (29) and are assigned to a polymerized form of formaldehyde (polyoxymethylene) adsorbed on silica (POM–Si) (22, 29).

Transient spectra were obtained after switching the feed from 3/1 H_2/CO to H_2 at a total pressure of 0.65 MPa while maintaining the temperature of the Cu/SiO_2 catalysts at 523 K. The results are shown in Fig. 3. In the C–H stretching region, all features decay slowly over the 24 h transient. After about 4 min, a feature at 3013 cm^{-1}(sh) becomes apparent due to gas phase methane (30). A small amount of methane formation has been previously observed by the present authors under these experimental conditions (14). The peaks for CH_3O–Cu (2939, 2878, 2830 cm^{-1}) decay at a similar rate to the features for CH_3O–Si (2962, 2861, and 1464 cm^{-1}), and POM–Si (1485 and 1377 cm^{-1}) is removed after 24 h in hydrogen.

ZrO_2/SiO_2 and $Cu/ZrO_2/SiO_2$

CO adsorption. Figure 4 shows spectra taken after ZrO_2/SiO_2 was exposed to He/CO at a ratio of 3/1 and a total pressure of 0.65 MPa for 90 min at temperatures between 323 and 523 K. At 323 K, features attributed to bidentate bicarbonate on ZrO_2 (b-HCO_3–Zr) (1607 and 1461 cm^{-1}) (18, 31–39), and carboxylate on ZrO_2 (CO_2^-–Zr) (1590 cm^{-1}) (34) are prevalent. Significant bidentate formate on ZrO_2 (b-HCOO–Zr) formation becomes evident at 423 K giving characteristic maxima at 2976, 2892, 1564, 1389, and 1370 cm^{-1} (17, 18, 31, 32, 36–38, 40–42). At 523 K, only b-HCOO–Zr is observable in the spectrum.

Figure 5 shows spectra obtained during the exposure of $Cu/ZrO_2/SiO_2$ to He/CO at a ratio of 3/1 and a total pressure of 0.65 MPa for 90 min at temperatures between 323 and 523 K. At 323 K, b-HCO_3–Zr (1607 cm^{-1}), CO_2^-–Zr (1584, 1425 cm^{-1}), and b-HCOO–Zr (2980, 2895, 1566, 1387, and 1371 cm^{-1}) are prevalent. At 523 K, b-HCOO–Zr is the dominant observable species in the spectrum. The b-HCOO–Zr band intensities decrease only moderately throughout the investigated temperature range. The feature at 1482 cm^{-1} is caused by monodentate carbonate on zirconia (m-CO_3–Zr) (18, 34–36, 38, 39, 41). The shoulder at 1354 cm^{-1} is caused by bidentate carbonate on zirconia (b-CO_3–Zr) (18, 31–33, 35, 36, 38, 39), but the companion feature at about 1567 cm^{-1} is obscured. The feature observable at 1505 cm^{-1} at 523 K is assigned to m-CO_3–Zr.

CO hydrogenation. Figure 6 shows spectra obtained while flowing H_2/CO at a ratio of 3/1 and a total pressure of 0.65 MPa at temperatures between 323 and 523 K over ZrO_2/SiO_2. Spectra were collected after 5 h at each temperature. The results are identical to those obtained during CO adsorption with regards to b-HCO_3–Zr, CO_2^-–Zr, and b-HCOO–Zr formation (see Fig. 4). However, during CO hydrogenation at 473 and 523 K, new features are observed at 2946 and 2846 cm^{-1}, which are attributed to methoxide species on ZrO_2 (CH_3O–Zr) (17, 18, 31, 32, 36, 37, 40, 41).

Figure 7 shows spectra obtained after exposure of $Cu/ZrO_2/SiO_2$ to flowing H_2/CO (3/1) at a total pressure of 0.65 MPa and temperatures between 323 and 523 K. Spectra

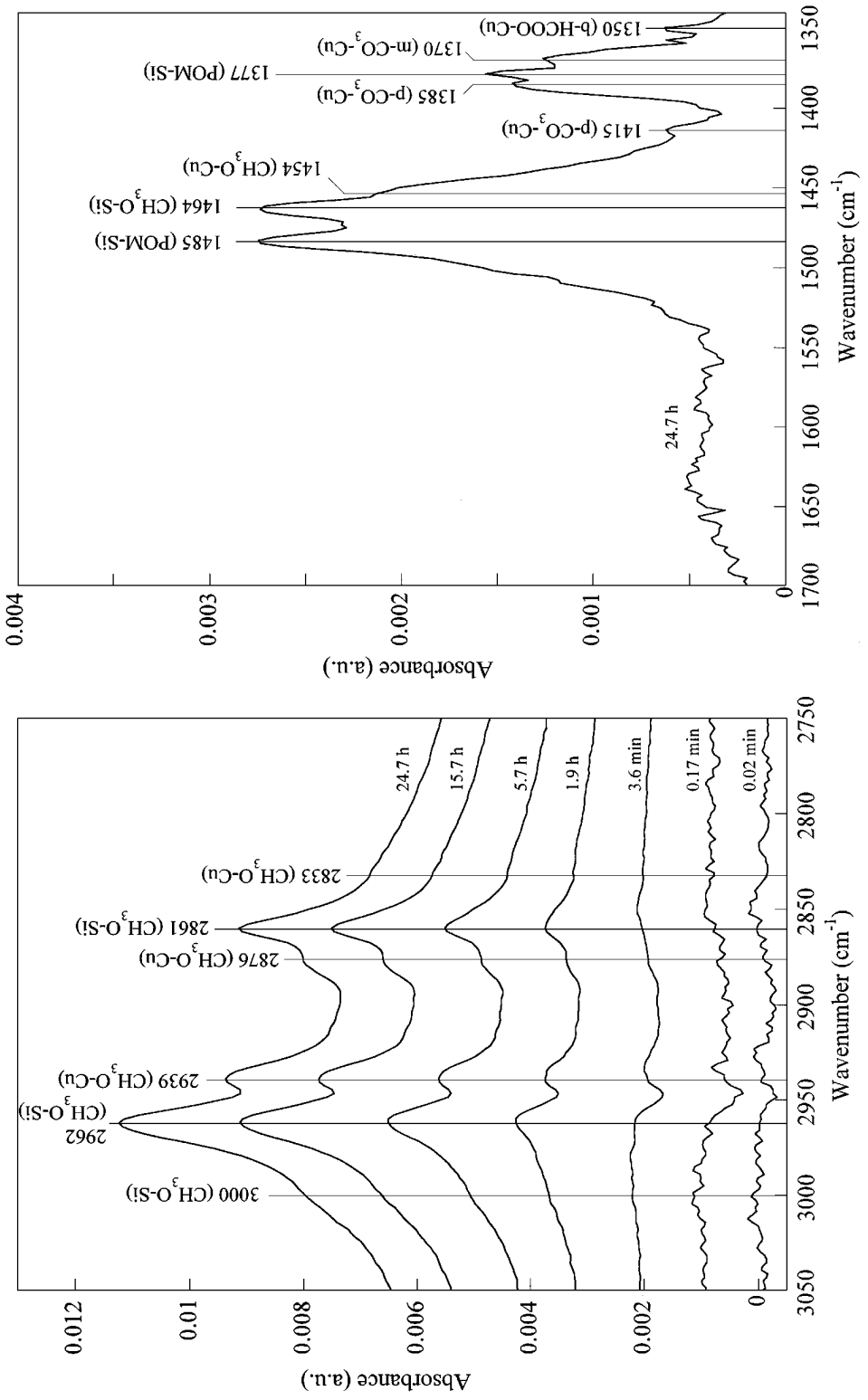

FIG. 2. Infrared spectra taken for Cu/SiO_2 at 523 K after switching feed from 0.65 MPa H_2 to 0.16 MPa CO and 0.49 MPa H_2 flowing at a total rate of 60 cm^3/min. Spectra referenced to Cu/SiO_2 under 0.65 MPa H_2 flow at 523 K.

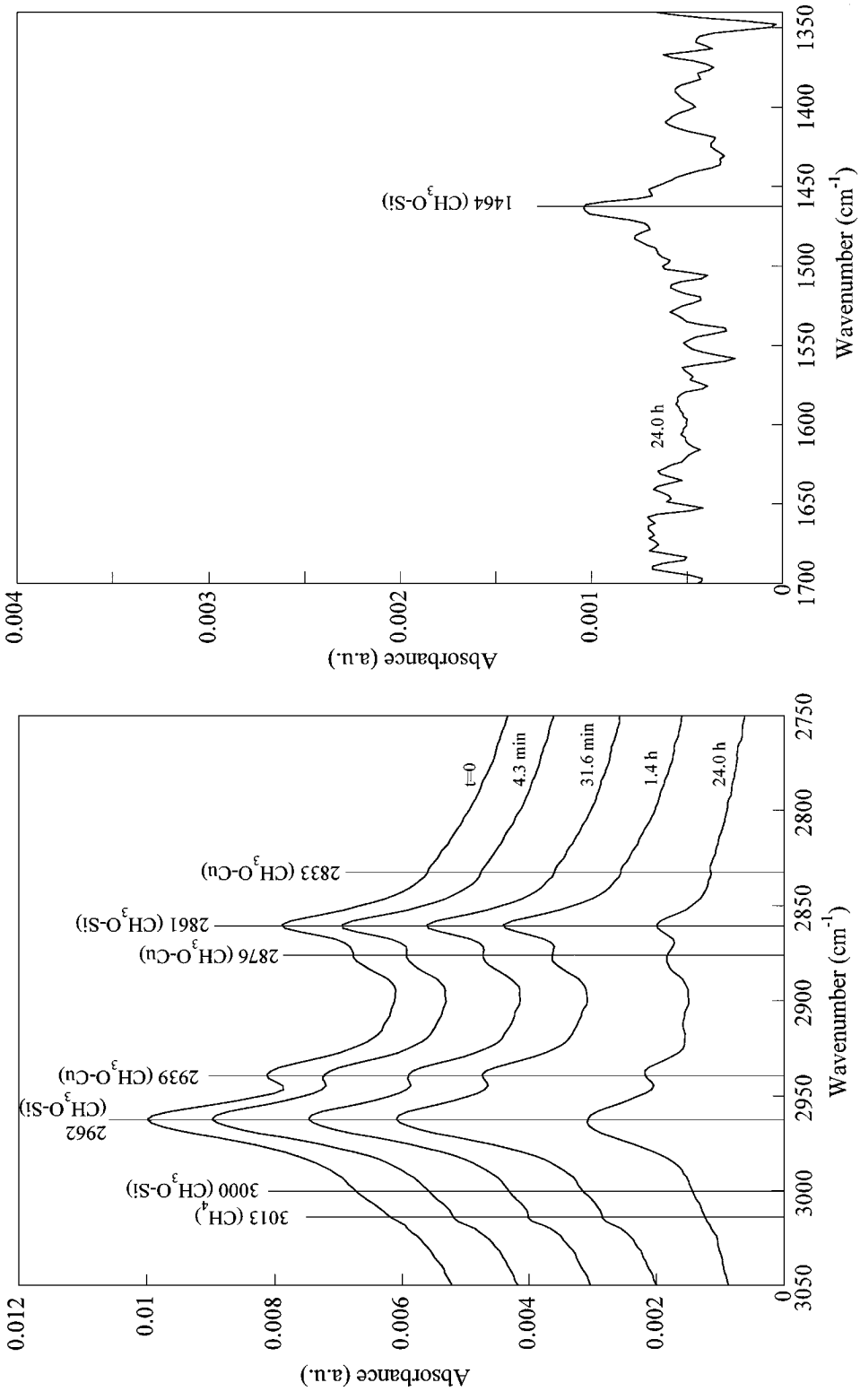

FIG. 3. Infrared spectra taken for Cu/SiO_2 at 523 K after switching feed from 0.16 MPa CO and 0.49 MPa H_2 to 0.65 MPa H_2 flowing at a total rate of 60 cm^3/min. Spectra referenced to Cu/SiO_2 under 0.65 MPa H_2 flow at 523 K.

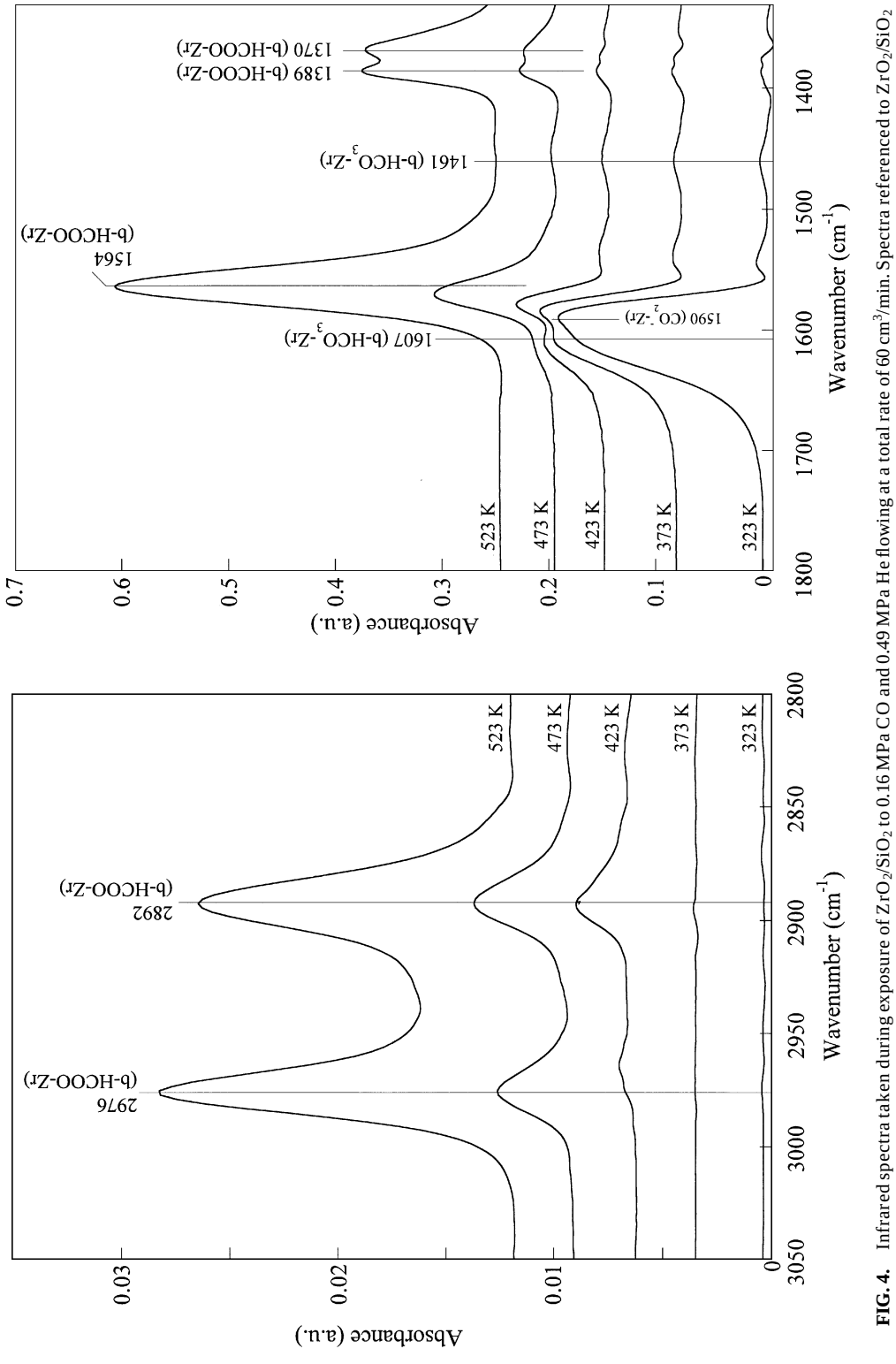

FIG. 4. Infrared spectra taken during exposure of ZrO_2/SiO_2 to 0.16 MPa CO and 0.49 MPa He flowing at a total rate of 60 cm^3/min. Spectra referenced to ZrO_2/SiO_2 under 0.65 MPa He flow at each temperature.

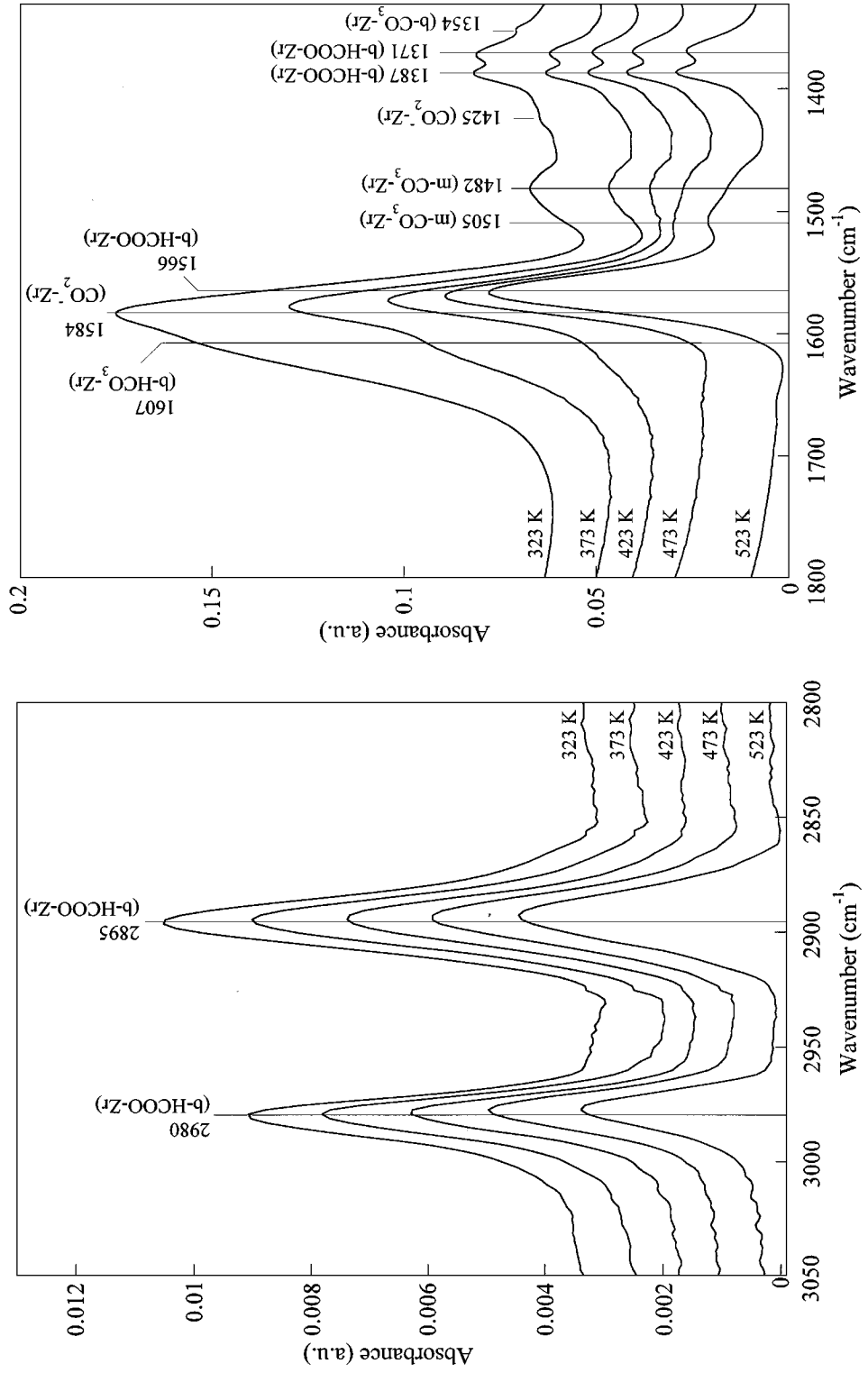

FIG. 5. Infrared spectra taken during exposure of $Cu/ZrO_2/SiO_2$ to 0.16 MPa CO and 0.49 MPa He flowing at a total rate of 60 cm^3/min. Spectra referenced to $Cu/ZrO_2/SiO_2$ under 0.65 MPa He flow at each temperature.

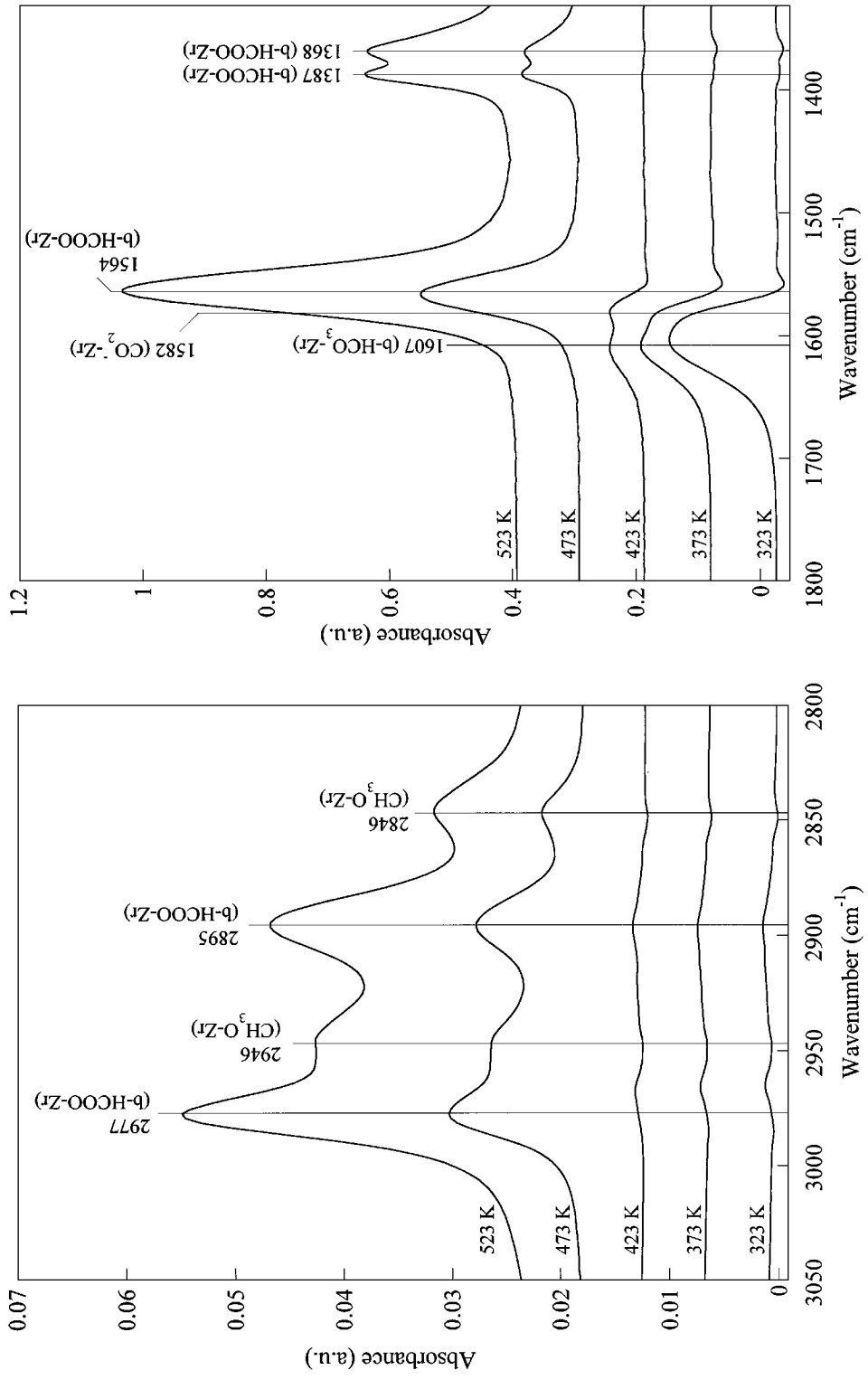

FIG. 6. Infrared spectra taken during exposure of ZrO_2/SiO_2 to 0.16 MPa CO and 0.49 MPa H_2 flowing at a total rate of 60 cm^3/min. Spectra referenced to ZrO_2/SiO_2 under 0.65 MPa H_2 flow at each temperature.

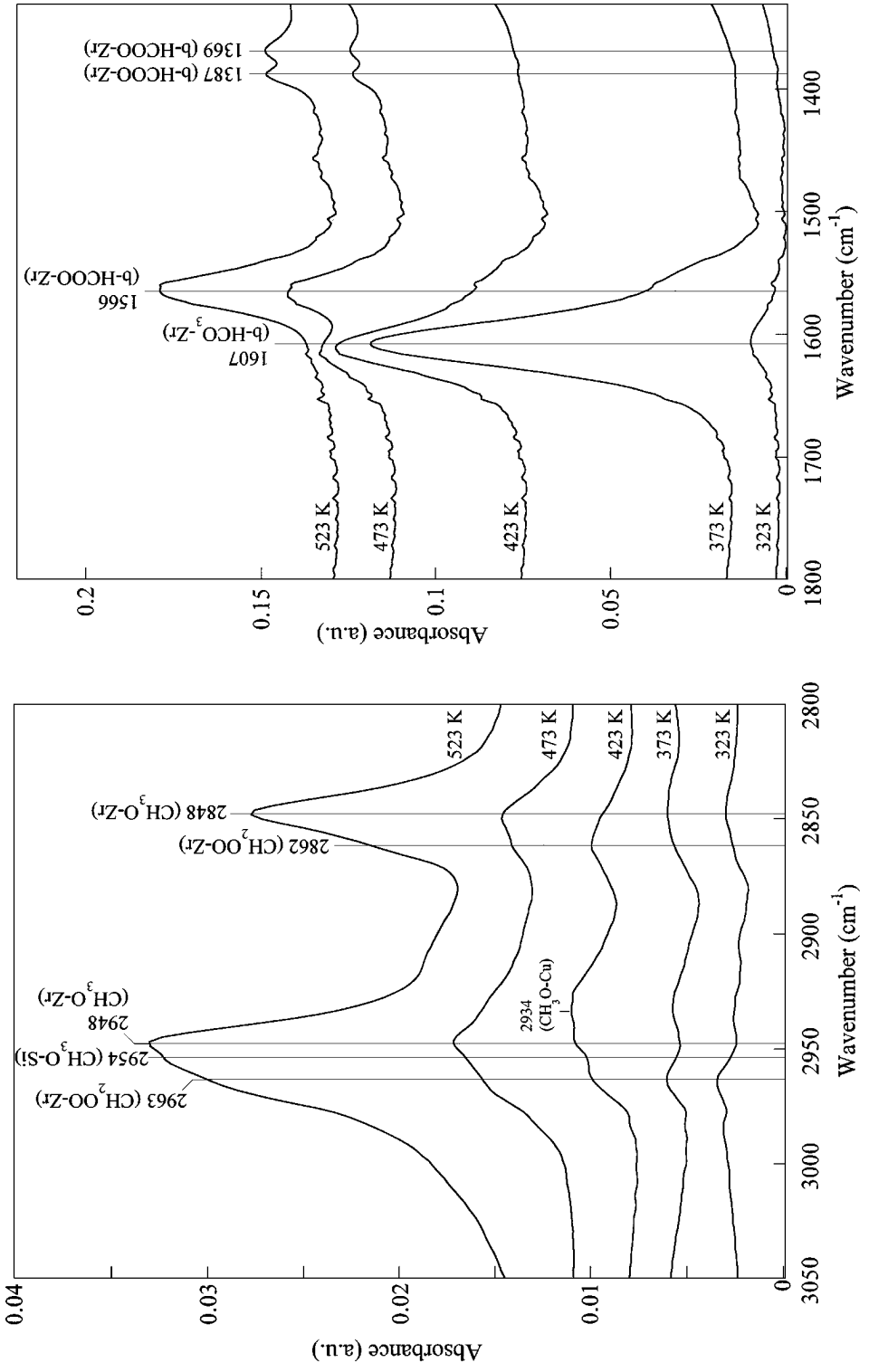

FIG. 7. Infrared spectra taken during exposure of $Cu/ZrO_2/SiO_2$ to 0.16 MPa CO and 0.49 MPa H_2 flowing at a total rate of 60 cm^3/min. Spectra referenced to $Cu/ZrO_2/SiO_2$ under 0.65 MPa H_2 flow at each temperature.

were collected after 5 h at each temperature. Between 323 and 423 K, b-HCO_3–Zr (1607 cm^{-1}) is the dominant species present, and the intensity of the band associated with this species goes through a maximum at 373 K. Significant concentrations of b-HCOO–Zr (1566, 1387, 1369 cm^{-1}) are not observed at temperatures below 473 K. At 423 K, features caused by bidentate methylenebisoxy on zirconia (b-CH_2OO–Zr, 2963, 2862 cm^{-1}) (18, 40, 43–46), CH_3O–Cu (2934 cm^{-1}), and CH_3O–Zr (2948, 2848 cm^{-1}) become observable. At higher temperatures, the peaks caused by CH_3O–Zr and CH_3O–Si (2954 cm^{-1}) dominate the spectra in the C–H stretching region. The b-HCOO–Zr features in the C–H stretching region are obscured by the relatively intense methoxide bands.

Temporal resolution of surface species. Transient spectra were obtained after switching the feed from 3/1 He/CO to 3/1 H_2/CO at a total pressure of 0.65 MPa while maintaining the temperature of the ZrO_2/SiO_2 catalyst at 523 K; they are shown in Fig. 8. At the beginning of the transient, only b-HCOO–Zr (2977, 2894, 1564, 1387, 1368 cm^{-1}) is present, and the intensities of the associated features do not change significantly during the 25 h transient. After about 3 h, features for CH_3O–Zr (2945 and 2843 cm^{-1}) become observable and increase in intensity during the remainder of the transient.

Transient spectra were obtained after switching the feed from 3/1 He/CO to 3/1 H_2/CO at a total pressure of 0.65 MPa while maintaining the temperature of the $Cu/ZrO_2/SiO_2$ catalyst at 523 K, and the results are shown in Fig. 9. At the beginning of the transient, only b-HCOO–Zr (2982, 2900, 1564, 1389, 1371 cm^{-1}) is present, and the intensities of the associated features decrease to nearly zero intensity during the 16 h transient. After about 5 min, features for CH_3O–Zr (2949 and 2849 cm^{-1}) and CH_3O–Si (2955 cm^{-1}) become observable and increase in intensity during the remainder of the transient. After about 35 min, a feature resulting from CH_2OO–Zr (2967 cm^{-1}) is apparent and increases in intensity during the remainder of the transient. At longer times, bands caused by CH_3O–Si are observable at 1461 and 3000 cm^{-1}, as is the feature caused by CH_3O–Zr at 1454 cm^{-1}. The shoulder at 2912 cm^{-1} is assigned to an overtone of the CH_3O–Zr band at 1454 cm^{-1}. It is observable only when the feature at 1454 cm^{-1} is intense and correlates with the appearance (see Fig. 9) and disappearance (see Fig. 13) of the feature at 1454 cm^{-1}.

The dynamics of the behavior of b-HCOO–Zr and CH_3O–Zr on ZrO_2/SiO_2 and $Cu/ZrO_2/SiO_2$ during the experiments presented in Figs. 8 and 9 are compared in Fig. 10. The peak intensity has been normalized to the value observed at the beginning of the transient for b-HCOO–Zr and to the value observed at the end of the transient for CH_3O–Zr. The apparent first-order rate coefficients for the appearance or disappearance of each species determined from the initial portion of the transient are given in the legend. It is evident that the surface concentration of b-HCOO–Zr is essentially unaffected upon switching from He/CO to H_2/CO for ZrO_2/SiO_2, but decreases relatively rapidly when the same experiment is conducted with $Cu/ZrO_2/SiO_2$. It is also observed that CH_3O–Zr forms much more rapidly in the presence of Cu and that the rate coefficient for the appearance of CH_3O–Zr is almost the same as the rate coefficient for b-HCOO–Zr consumption on $Cu/ZrO_2/SiO_2$.

Figure 11 shows the evolution of gas phase methanol as a function of time upon switching the feed to the microreactor from He/CO to H_2/CO at 523 K. The methanol signal was measured by following the intensity of the signal at $m/e = 31$. Separate tests reveal that the response of the analytical system to a step change in methanol concentration in the product stream is rapid compared to the dynamics observed in Fig. 11. Also shown in Fig. 11 is the intensity of the band at 2849 cm^{-1} for CH_3O–Zr measured as a function of time in the same experiment. The data show very clearly that the appearance of methanol in the gas phase is strongly correlated with the appearance of CH_3O–Zr on the surface of zirconia.

Transient spectra were obtained after switching the feed from 3/1 H_2/CO to H_2 at a total pressure of 0.65 MPa while maintaining the temperature of the ZrO_2/SiO_2 catalyst at 523 K. The results are shown in Fig. 12. Features caused by b-HCOO–Zr decay very slowly over the 119 h transient. Features caused by CH_3O–Zr increase in intensity slightly during the first 15 h of the transient and then decay slowly and persist even after 119 h.

Figure 13 shows transient spectra obtained after switching the feed from 3/1 H_2/CO to H_2 at a total pressure of 0.65 MPa while maintaining the temperature of the $Cu/ZrO_2/SiO_2$ catalyst at 523 K. In the C–H stretching region, all features decay at similar rates during the 29 h transient. In the region 1800–1350 cm^{-1}, b-HCOO–Zr is absent at the beginning of the transient. The feature at 1536 cm^{-1} is assignable to b-CO_3–Zr, the feature at 1410 cm^{-1} to CO_3–Cu, the feature at 1461 cm^{-1} to CH_3O–Si, and the feature at 1454 cm^{-1} to CH_3O–Zr. The shoulders observed at 2912 and 2995 cm^{-1} are assigned to CH_3O–Zr and CH_3O–Si, respectively (see Fig. 9). All features in this region decay slowly during the transient with CO_3–Cu being the most persistent.

Figure 14 compares the dynamics for the consumption of b-HCOO–Zr and CH_3O–Zr on ZrO_2/SiO_2 and CH_3O–Zr consumption on $Cu/ZrO_2/SiO_2$ when the feed is switched from H_2/CO to H_2 at 523 K and a total pressure of 0.65 MPa (Figs. 12 and 13). Shown are the peak intensities for b-HCOO–Zr and CH_3O–Zr normalized to their maximum intensities observed at the beginning of the transient. Also shown is the apparent first-order rate constant for CH_3O–Zr decay on both catalysts and for the decay of b-HCOO–Zr on ZrO_2/SiO_2. The result shows that the

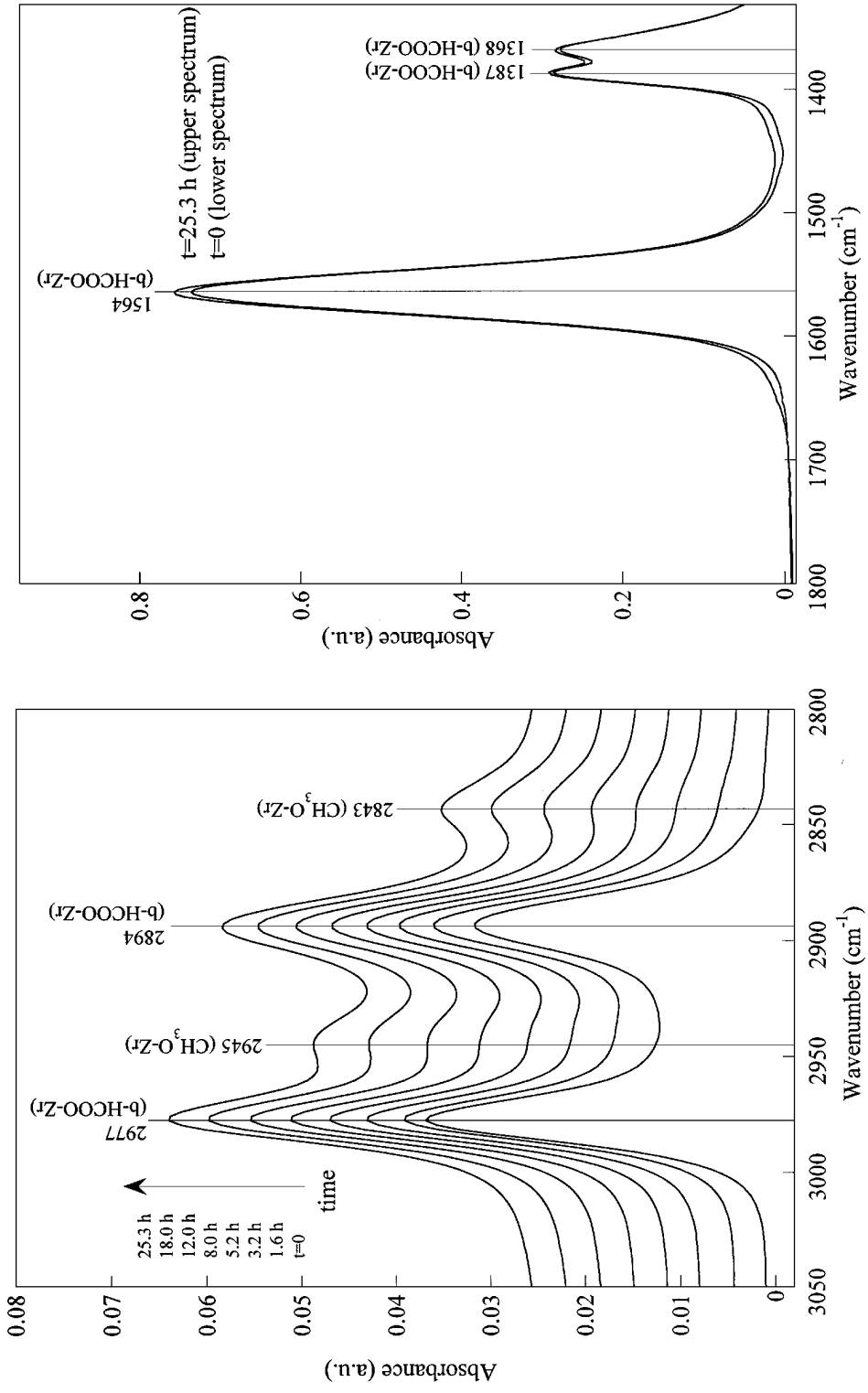

FIG. 8. Infrared spectra taken for ZrO_2/SiO_2 at 523 K after switching feed from 0.49 MPa He and 0.16 MPa CO to 0.49 MPa H_2 and 0.16 MPa CO flowing at a total rate of 60 cm^3/min. Flow switched after 2 h in He/CO. Spectra referenced to ZrO_2/SiO_2 under 0.65 MPa H_2 flow at 523 K.

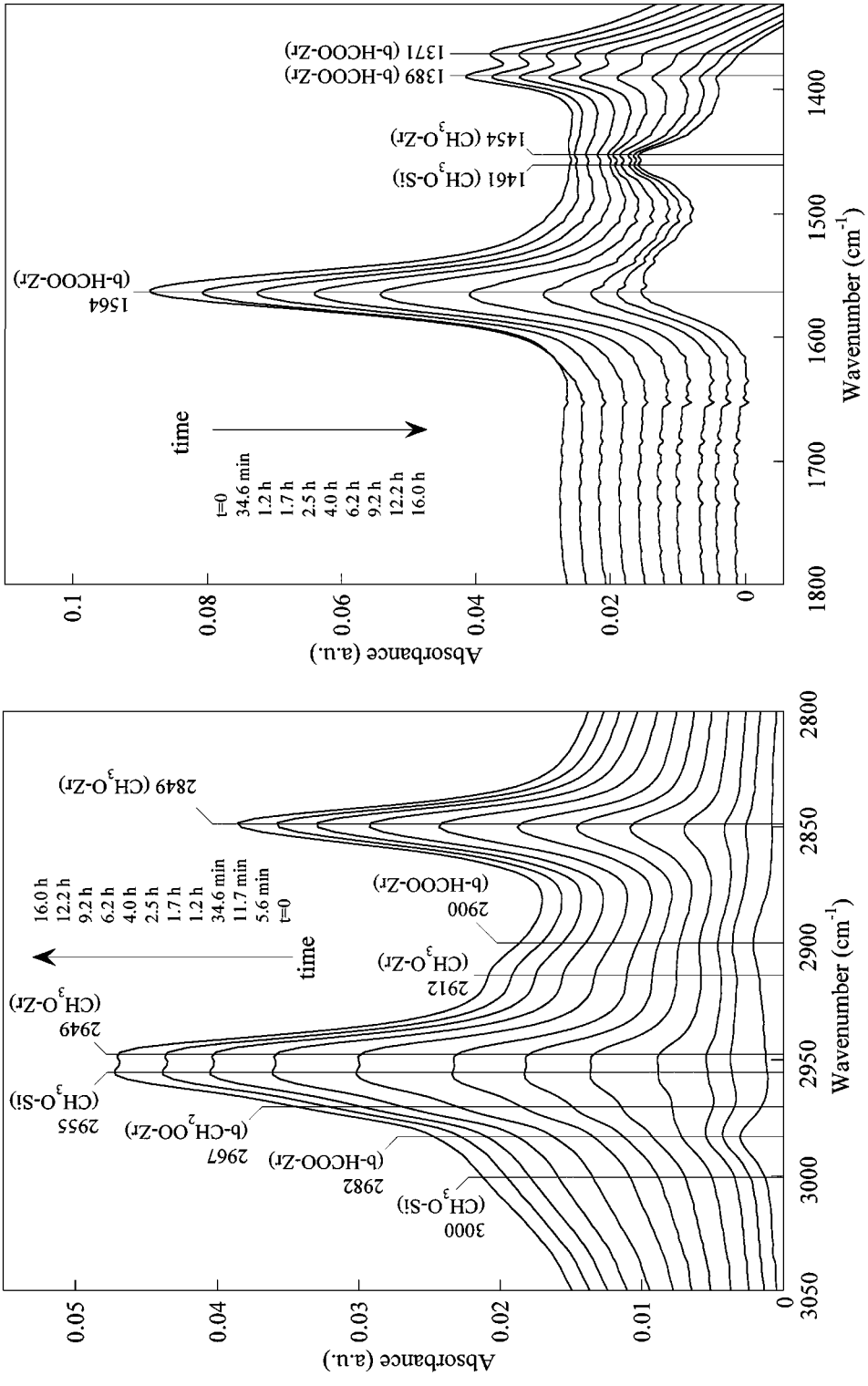

FIG. 9. Infrared spectra taken for $Cu/ZrO_2/SiO_2$ at 523 K after switching feed from 0.49 MPa He and 0.16 MPa CO to 0.49 MPa H_2 and 0.16 MPa CO flowing at a total rate of 60 cm^3/min. Flow switched after 2 h in He/CO. Spectra referenced to $Cu/ZrO_2/SiO_2$ under 0.65 MPa H_2 flow at 523 K.

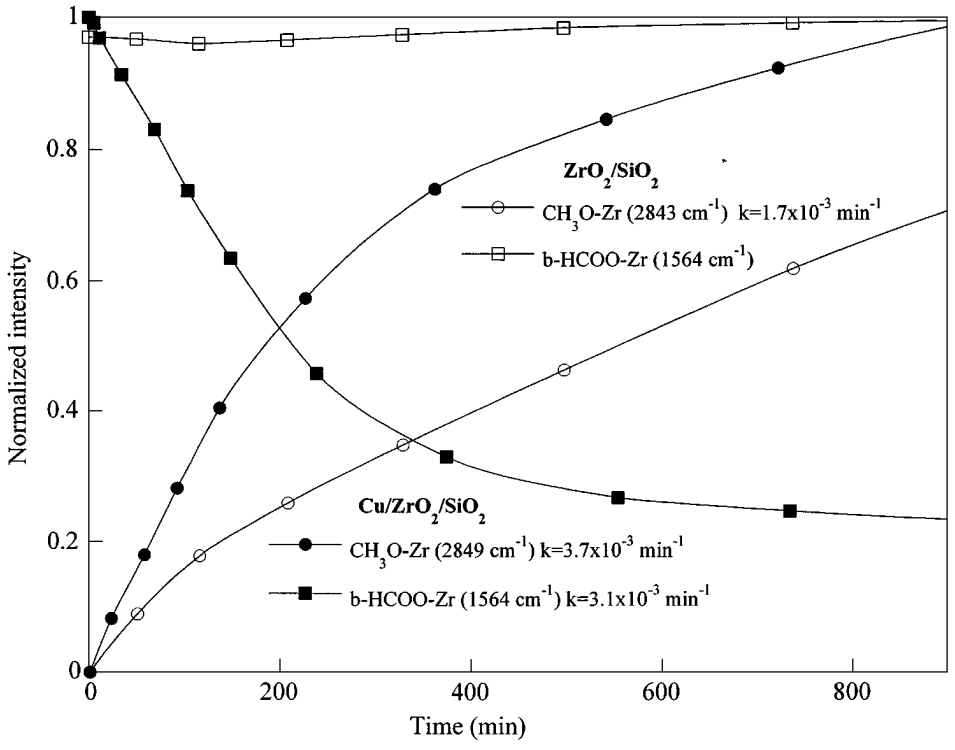

FIG. 10. Intensities of b-HCOO−Zr and CH_3O−Zr features for both ZrO_2/SiO_2 and $Cu/ZrO_2/SiO_2$ during the experiments in Figs. 8 and 9. Intensities normalized to those observed at the beginning of the transient for b-HCOO−Zr and to the value observed at the end of the transient for CH_3O−Zr.

concentration of methoxide decays much more rapidly for $Cu/ZrO_2/SiO_2$ than for ZrO_2/SiO_2. For both catalysts, the methoxide concentration goes through a maximum. The time at which the maximum appears and its intensity are significantly lower for $Cu/ZrO_2/SiO_2$ than ZrO_2/SiO_2, consistent with the more rapid removal of methoxide species from the Cu-containing catalyst.

Comparison of methanol synthesis from H_2/CO and H_2/CO_2. Figure 15 compares spectra taken during methanol synthesis from H_2/CO and H_2/CO_2 (18) at 523 K and a total pressure of 0.65 MPa. With the exception of the feed composition, the reaction conditions in both experiments are the same. The measured rate of methanol synthesis from H_2/CO_2 is 3.5 times higher than that from H_2/CO under these conditions, and it is observed that the rate of methanol synthesis from H_2/CO_2 is always higher than that from H_2/CO at comparable conditions. Figure 15 shows that even though the intensities of the bands for methoxide species on zirconia are comparable in both reaction mixtures, the intensities of the bands for formate species on zirconia are 22 times higher for the hydrogenation of CO_2.

DISCUSSION

As noted in the introduction, studies by a number of investigators have demonstrated that Cu catalysts containing zirconia are exceptionally active for methanol synthesis from both CO_2 and CO (2, 4–14). Likewise, the results presented in Table 1 and those previously reported by the present authors, show that the addition of zirconia to Cu/SiO_2 greatly enhances the activity of the catalyst for methanol synthesis from CO (14). Therefore, it is of interest to consider the ways in which the presence of zirconia either as a support or an additive enhances the rate of methanol synthesis. The first possibility is that zirconia acts independently of copper because zirconia is known to be a catalyst for the synthesis of methanol (40, 47). This interpretation can be quickly ruled out because ZrO_2 exhibits no measurable activity for methanol synthesis from CO under the conditions of the present study (14). The second possibility is that zirconia promotes the rate of methanol formation occurring on the surface of Cu or alternatively that Cu promotes the synthesis of methanol over zirconia. Which of these latter two options offers the most plausible explanation requires a consideration of the observables.

It has been previously reported that on Cu/SiO_2, the only plausible route to methanol formation is via the stepwise hydrogenation of CO to form formyl, formaldehyde, and then methoxide species, the final precursor to methanol (48). Methanol is then formed via reductive elimination of the methoxide species. Figure 2 shows that most of the species observed during methanol synthesis from CO/H_2

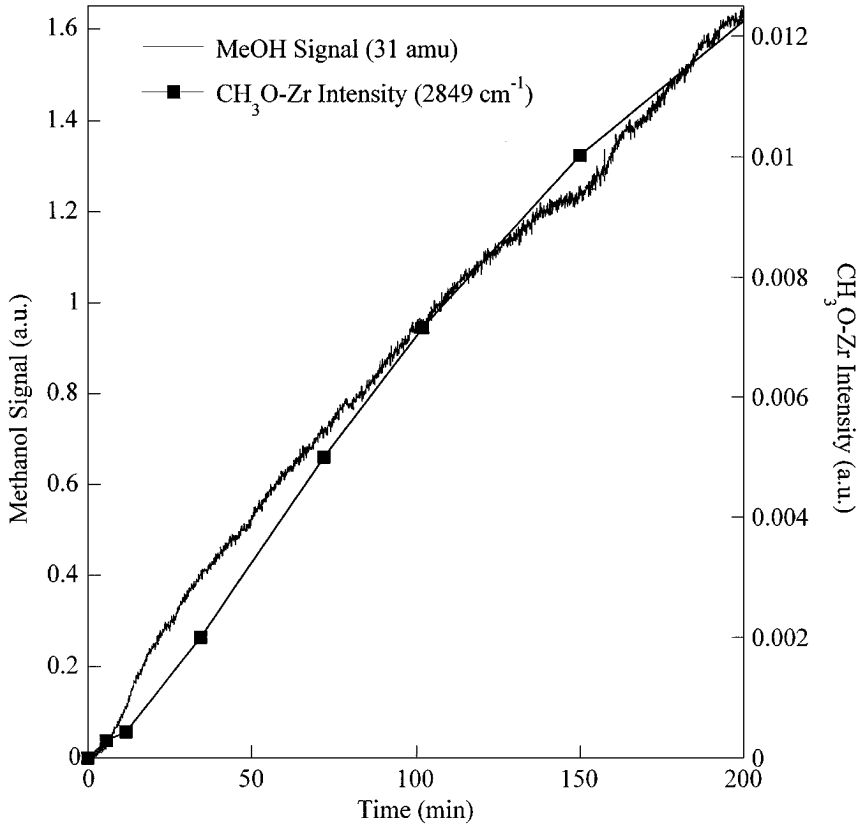

FIG. 11. Methanol signal observed at $m/e = 31$ and the intensity of the band at 2849 cm^{-1} for CH_3O–Zr as functions of time upon switching the reactor feed from 0.49 MPa He and 0.16 MPa CO to 0.49 MPa H_2 and 0.16 MPa CO at 523 K and a total flow rate of 60 cm^3/min. The flow was switched after 2 h in He/CO. The catalyst is $Cu/ZrO_2/SiO_2$.

on Cu/SiO_2 are present on Cu. By contrast, Figs. 7, 9, and 13 show that during CO hydrogenation over $Cu/ZrO_2/SiO_2$, virtually all the observable adsorbed species occur on ZrO_2. The presence of Cu lowers the temperature at which formate is formed from CO (323 K for $Cu/ZrO_2/SiO_2$ versus 423 K for ZrO_2/SiO_2). This is attributed to the adsorption of CO on Cu (Fig. 1), which subsequently spills over to zirconia and reacts with hydroxyl groups on zirconia to form formate species on zirconia. In the absence of Cu, this mechanism for low-temperature formate formation is unavailable, and formate is formed only at higher temperatures via the direct interaction of CO with hydroxyl groups on zirconia. The presence of Cu also lowers the temperature at which CH_3O–Zr species are first observed (423 K for $Cu/ZrO_2/SiO_2$ versus 473 K for ZrO_2/SiO_2). As shown in Fig. 10, the presence of Cu also enhances the rate of hydrogenation of b-HCOO–Zr and the rate of CH_3O–Zr formation, as well as the rate of reductive elimination of CH_3O–Zr (see Fig. 14).

Because atomic hydrogen is required for the hydrogenation of b-HCOO–Zr and the reductive elimination of CH_3O–Zr and because Cu is more effective than ZrO_2 in dissociating H_2 (49), the previously noted observations suggest that Cu is responsible for supplying the atomic hydrogen required for the hydrogenation reactions occurring on ZrO_2. Previous work on Cu/SiO_2 has shown that H_2 adsorbs dissociatively on Cu with a heat of adsorption of about 12 kcal/mol and an activation barrier of about 10.5 kcal/mol (50). Thus, it seems reasonable to suggest that $Cu/ZrO_2/SiO_2$ acts as a bifunctional catalyst. The Cu serves to adsorb H_2 dissociatively and to provide a source of atomic hydrogen by spillover. Cu also appears to supply adsorbed CO to ZrO_2, aiding in the formation of formate on ZrO_2 at lower temperatures than on zirconia by itself. ZrO_2 serves to adsorb CO as carboxylate, bicarbonate, and formate species which then undergo stepwise hydrogenation to methanol. Additional methanol is probably formed over Cu itself as evidenced by the presence of methoxide on Cu (Fig. 7). A similar view of methanol synthesis over $Cu/ZrO_2/SiO_2$ has been suggested recently by the present authors (14, 18) and has been proposed by Bianchi *et al.* (41). The processes envisioned to occur on ZrO_2 are similar to those proposed to explain methanol synthesis on zirconia (40, 47), and attention has been drawn recently to the importance of hydrogen spillover during methanol synthesis on Cu/ZnO (51) and Pd/SiO_2 (52).

Based on the preceding arguments, a possible mechanism for CO hydrogenation to methanol in the presence of Cu

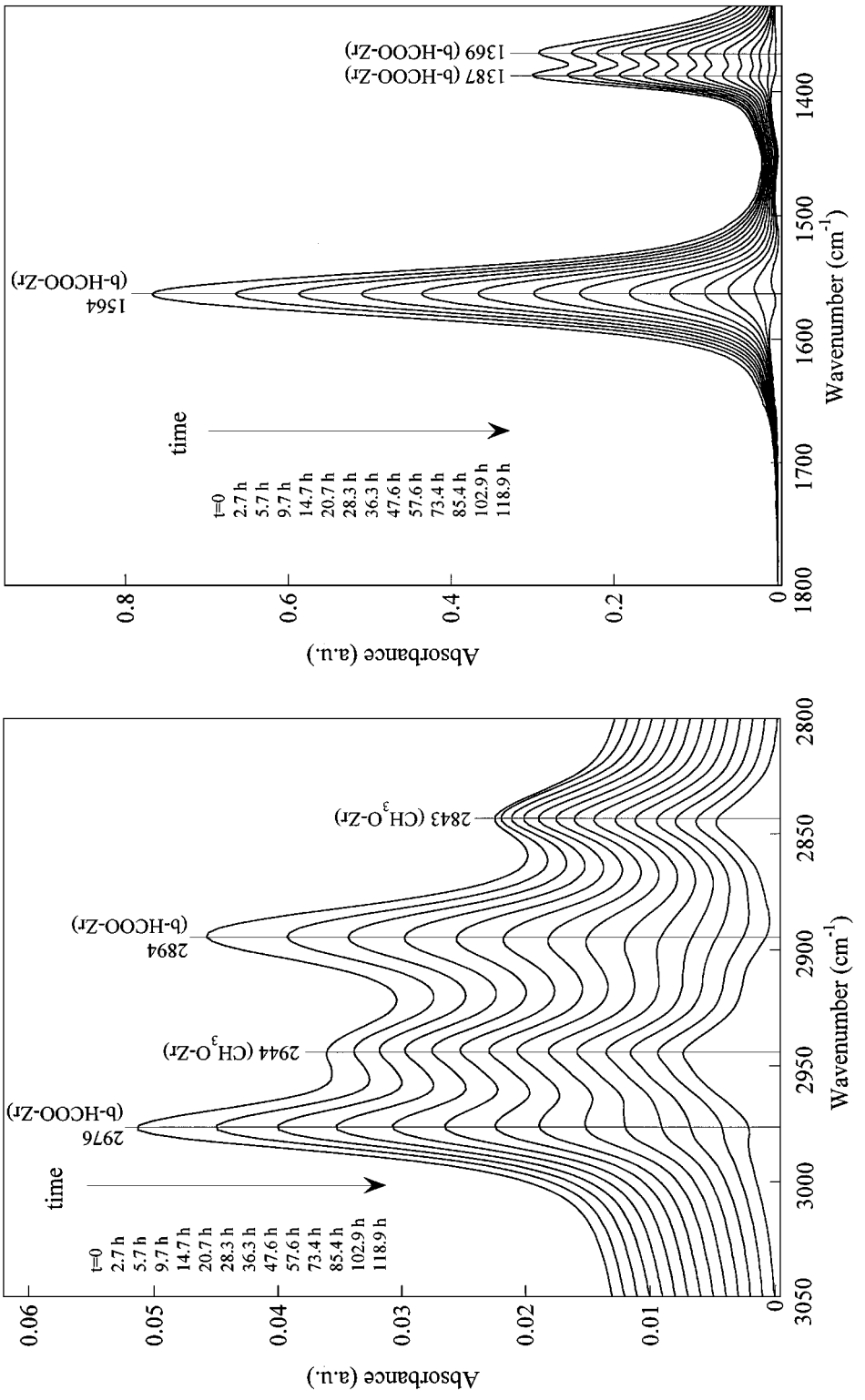

FIG. 12. Infrared spectra taken for ZrO_2/SiO_2 at 523 K after switching feed from 0.49 MPa H_2 and 0.16 MPa CO to 0.65 MPa H_2 flowing at a total rate of 60 cm^3/min. Flow switched after 21 h in H_2/CO. Spectra referenced to ZrO_2/SiO_2 under 0.65 MPa H_2 flow at 523 K.

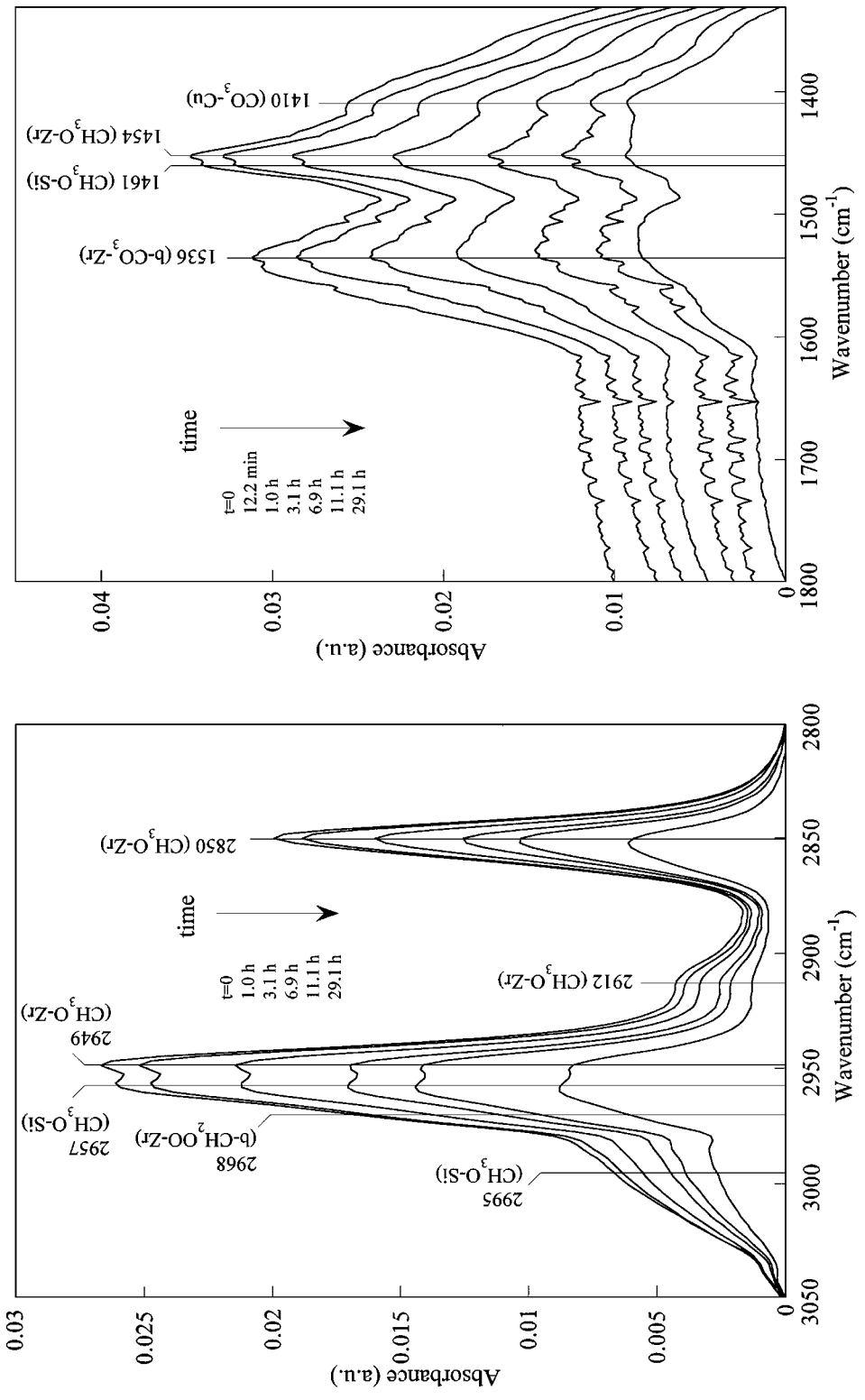

FIG. 13. Infrared spectra taken for $Cu/ZrO_2/SiO_2$ at 523 K after switching feed from 0.49 MPa H_2 and 0.16 MPa CO to 0.65 MPa H_2 flowing at a total rate of 60 cm^3/min. Flow switched after 20 h in H_2/CO. Spectra referenced to $Cu/ZrO_2/SiO_2$ under 0.65 MPa H_2 flow at 523 K.

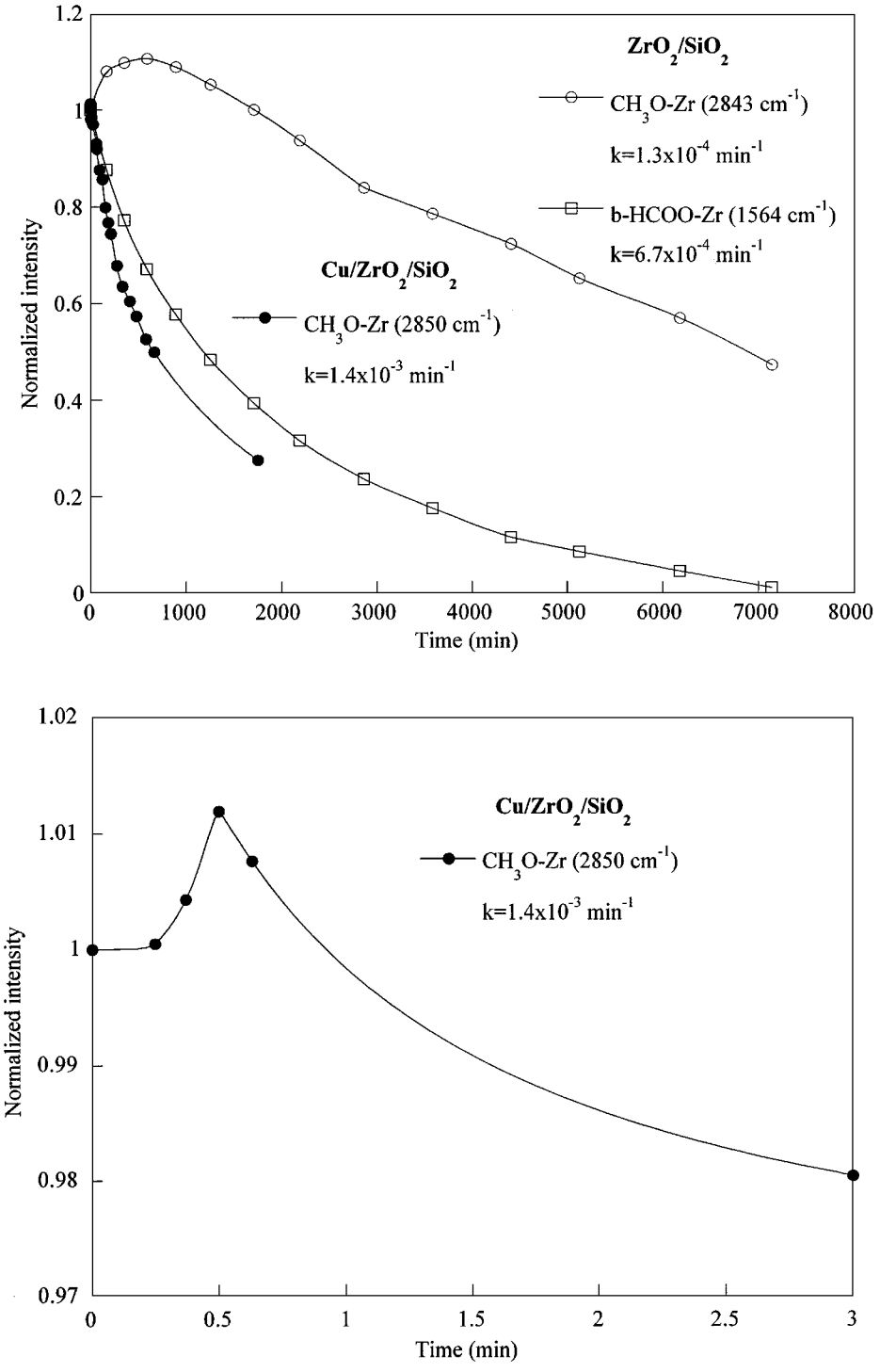

FIG. 14. Intensities of b-HCOO−Zr and CH_3O−Zr features for both ZrO_2/SiO_2 and $Cu/ZrO_2/SiO_2$ during the experiments in Figs. 12 and 13. Intensities normalized to those observed at the beginning of the transient.

and zirconia is offered in Fig. 16. In this scheme, Cu and ZrO_2 are envisioned to be in close proximity. CO adsorption leads to either carboxylate or formate species on zirconia. Formate species are formed by the interaction of CO with OH groups on zirconia, whereas carboxylate species are formed by the interaction of CO with O^{2-} anions on the ZrO_2. Carboxylate species react with OH groups on zirconia to form bicarbonate species which may be converted to formate (18). Formate species on zirconia are also formed by reaction of CO spilled over from Cu with OH groups on

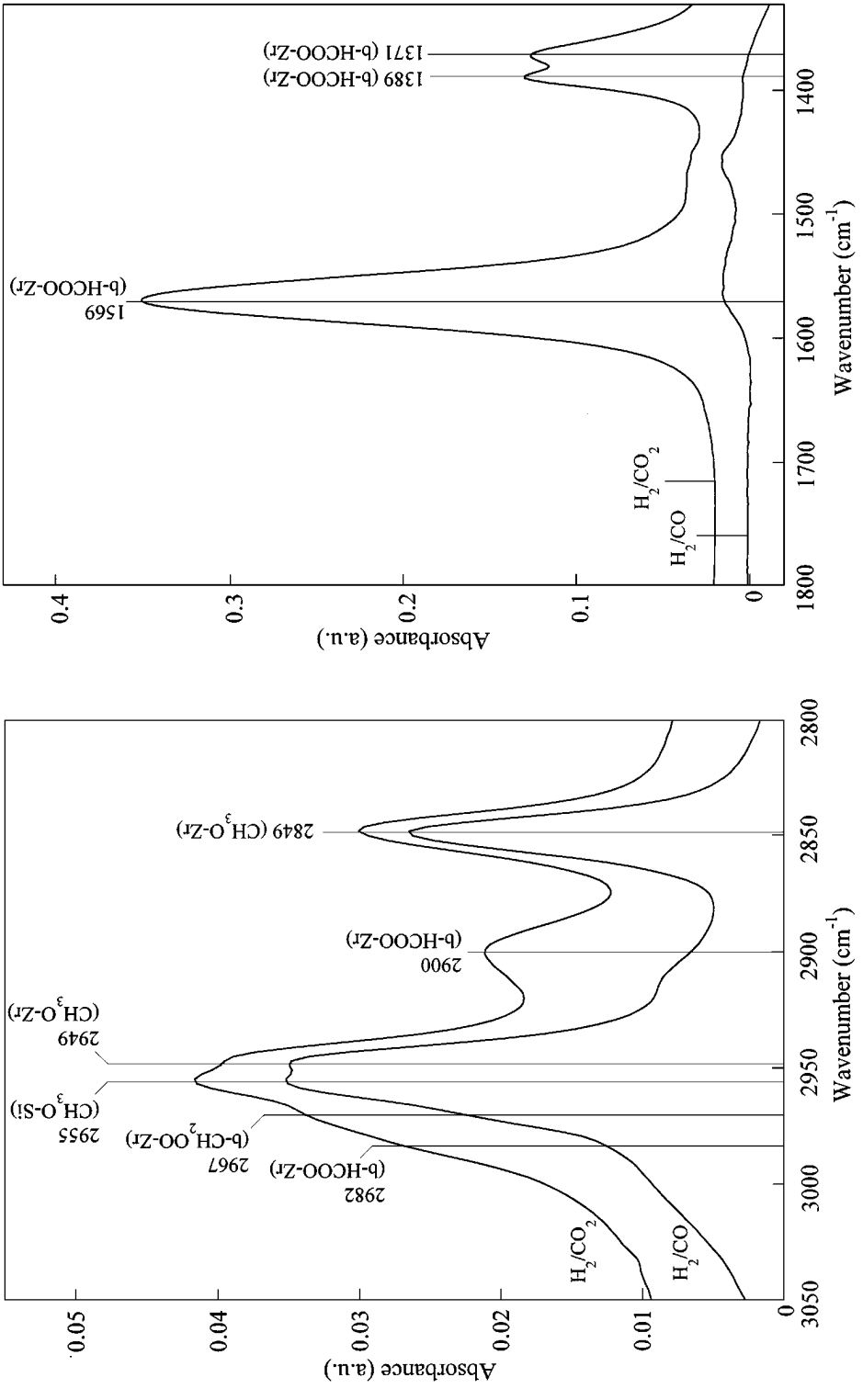

FIG. 15. Infrared spectra taken during exposure of $Cu/ZrO_2/SiO_2$ to 0.16 MPa CO and 0.49 MPa H_2 (bottom spectrum) flowing at a total rate of 60 cm^3/min for 16 h at 523 K and during exposure of $Cu/ZrO_2/SiO_2$ to 0.16 MPa CO_2 and 0.49 MPa H_2 [top spectrum (18)] flowing at a total rate of 60 cm^3/min for 16 h at 523 K. Both spectra referenced to $Cu/ZrO_2/SiO_2$ under 0.65 MPa H_2 flow at 523 K.

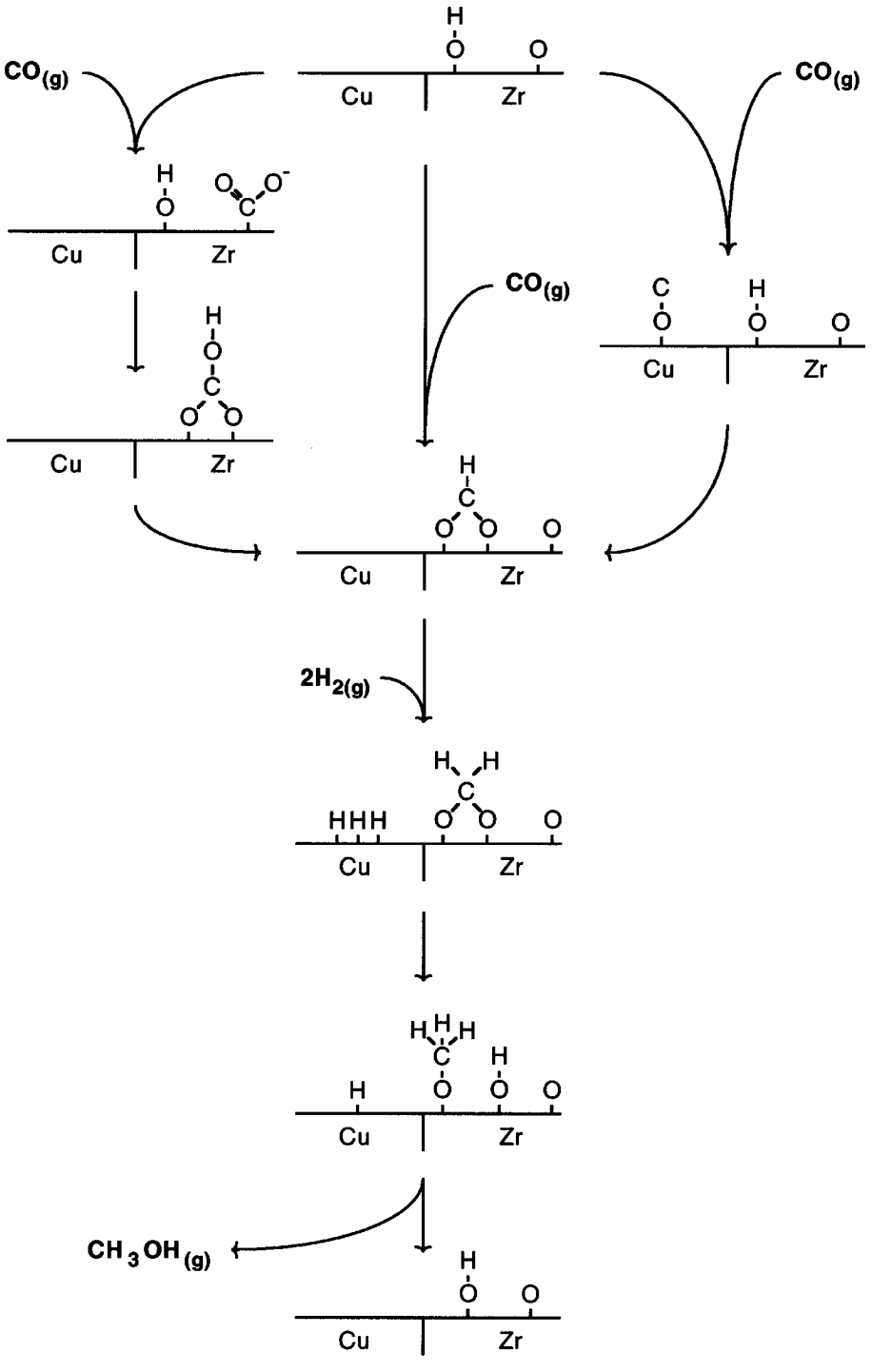

FIG. 16. Proposed mechanism for the synthesis of methanol from CO and H_2 on Cu- and ZrO_2-containing catalysts.

zirconia, as evidence by the enhanced formate formation in the presence of Cu (see Figs. 4 and 5).

Our previous studies have shown that under reaction conditions identical to those used here and with the same catalyst, the rate for methanol formation is insignificant below 423 K (14). Consistent with this, the in situ infrared spectra presented in Fig. 7 show that methoxide species are not formed in significant concentration below this temperature, during CO hydrogenation on $Cu/ZrO_2/SiO_2$. The concurrent appearance of bands for methylenebisoxy and methoxide species strongly supports the proposal that the former species is an intermediate in the conversion of b-HCOO–Zr

to CH_3O–Zr. The appearance of gas-phase methanol correlates strongly with the appearance of CH_3O–Zr (see Fig. 11), supporting the proposal that methoxide species on zirconia are the precursors to methanol.

The nature of the rate-determining step in the proposed mechanism can be deduced from the transient-response experiments presented in Figs. 9, 10, and 14. It is interesting to note that b-HCOO–Zr is largely absent on $Cu/ZrO_2/SiO_2$ during CO hydrogenation at 523 K at long times, but the intensities of the CH_3O–Zr features are high at these conditions (Fig. 9). It is also important to observe that both in the absence and presence of Cu, the surface concentration of CH_3O–Zr passes through a maximum when the feed to the catalyst is switched from H_2/CO to H_2 (see Fig. 14). However, the methoxide maximum occurs much sooner in the presence of Cu. If methoxide removal with hydrogen were fast compared to its formation from formate, this maximum would not be observed. These results suggest that the transformation of formate to methoxide occurs more readily than the conversion of methoxide to methanol and that the later reaction may be the difficult step along the route to gas-phase methanol.

Even though the release of methoxide species as methanol appears to be the slow step for methanol synthesis from H_2/CO, methoxide conversion is facile during CO_2 hydrogenation to methanol. During CO_2 hydrogenation, water is formed along with methanol, as well as via the RWGS reaction, whereas during CO hydrogenation water is not formed. Our previous work has shown that the hydrolysis of methoxide is extremely rapid in comparison to the rate of methoxide hydrogenation (18). Hence, during CO_2 hydrogenation, methoxide hydrolysis occurs readily, and methoxide conversion is not the slow step in methanol synthesis. During CO hydrogenation, methoxide conversion by hydrolysis is inoperative, and the slow conversion of methoxide by hydrogenation occurs. Therefore, CO and CO_2 hydrogenation to methanol appear to have different rate-determining steps, although the mechanism for methanol formation is similar in both cases. Because the methoxide surface concentration is observed to be comparable for both CO and CO_2 hydrogenation (see Fig. 15), the preceding argument suggests that the rate-determining step for CO_2 hydrogenation to methanol is necessarily faster than that for CO hydrogenation, and that the experimental observation that the rate of methanol synthesis is higher from H_2/CO_2 than for H_2/CO under the same reaction conditions (14) is justified. A similar suggestion has been made for methanol synthesis on Cu/ZnO (53).

As shown in Table 1, the methanol synthesis activity of $Cu/ZrO_2/SiO_2$ is 59 and 120 times that of Cu/SiO_2 when compared on a per mass and per copper site basis, respectively. This difference may be attributed to a change in the reaction pathway from a formyl mechanism for Cu/SiO_2 to a formate mechanism for $Cu/ZrO_2/SiO_2$. In support of this conclusion, we note that the apparent activation energy for methanol synthesis under the conditions of the present study is 5 kcal/mol lower for $Cu/ZrO_2/SiO_2$ as compared to Cu/SiO_2 (14). The present infrared results also indicate that formate species are involved in the synthesis of methanol on $Cu/ZrO_2/SiO_2$ but not on Cu/SiO_2.

CONCLUSIONS

The locus of methanol synthesis and the surface species formed from CO/H_2 over Cu/SiO_2 and $Cu/ZrO_2/SiO_2$ are found to be quite different. In the former case, the hydrogenation of CO to methanol occurs on Cu. Adsorbed CO on Cu undergoes sequential hydrogenation to methoxide species adsorbed on Cu and finally to methanol. For $Cu/ZrO_2/SiO_2$, virtually all the adsorbed species are associated with ZrO_2. CO adsorbs and forms carboxylate, bicarbonate, and formate, which then react with atomic hydrogen to form methoxide species, all of which are adsorbed on ZrO_2. The presence of Cu in $Cu/ZrO_2/SiO_2$ results in formate and methoxide formation at lower temperatures and higher rates, and increases the rate of reductive elimination of methoxide species as methanol. A bifunctional mechanism for methanol synthesis from CO/H_2 is proposed (see Fig. 16) in which formate species form on zirconia and undergo stepwise hydrogenation to methylenebisoxy, methoxide, and finally methanol,with atomic hydrogen being supplied by spillover from Cu. The reductive elimination of methoxide is slow relative to other steps in the reaction mechanism. The suppressed rate of methanol synthesis from CO as compared to CO_2 hydrogenation is ascribed to the absence of water formation, which prevents the more facile release of methoxide by hydrolysis. The enhanced rate of methanol synthesis from CO hydrogenation on $Cu/ZrO_2/SiO_2$ as compared to Cu/SiO_2 is attributed to the reaction proceeding through the lower energy formate route on $Cu/ZrO_2/SiO_2$, while proceeding through the higher energy formyl mechanism on Cu/SiO_2.

ACKNOWLEDGMENTS

The authors would like to acknowledge Hee-Chul Woo and Johan Agrell for their assistance with these studies. This work was supported by the Director, Office of Basic Energy Sciences, Chemical Sciences Division, of the U.S. Department of Energy under Contract DE-AC03-76SF00098.

REFERENCES

1. Klier, K., *Adv. Catal.* **31**, 243 (1982).
2. Bartley, G. J. J., and Burch, R., *Appl. Catal.* **43**, 141 (1988).
3. Robinson, W. R. A. M., and Mol, J. C., *Appl. Catal.* **44**, 165 (1988).
4. Denise, B., and Sneeden, R. P. A., *Appl. Catal.* **28**, 235 (1986).
5. Chen, H. W., White, J. M., and Ekerdt, J. G., *J. Catal.* **99**, 293 (1986).
6. Amenomiya, Y., *Appl. Catal.* **30**, 57 (1987).
7. Denise, B., Sneeden, R. P. A., Beguin, B., and Cherifi, O., *Appl. Catal.* **30**, 353 (1987).

8. Koeppel, R. A., Baiker, A., Schild, C., and Wokaun, A., *in* "Preparation of Catalysts V," Stud. Surf. Sci. Catal., Vol. 63, p. 59. (G. Poncelet, P. A. Jacobs, P. Grange, and B. Delmon, Eds.). Elsevier, Amsterdam, 1991.
9. Kanoun, N., Astier, M. P., and Pajonk, G. M., *Catal. Lett.* **15**, 231 (1992).
10. Koeppel, R. A., Baiker, A., and Wokaun, A., *Appl. Catal. A* **84**, 77 (1992).
11. Sun, Y., and Sermon, P. A., *J. Chem. Soc., Chem. Commun.* 1242 (1993).
12. Nitta, Y., Suwata, O., Ikeda, Y., Okamoto, Y., and Imanaka, T., *Catal. Lett.* **26**, 345 (1994).
13. Sun, Y., and Sermon, P. A., *Catal. Lett.* **29**, 361 (1994).
14. Fisher, I. A., Woo, H. C., and Bell, A. T., *Catal. Lett.* **44**, 11 (1997).
15. Schild, C., Wokaun, A., and Baiker, A., *J. Mol. Catal.* **63**, 243 (1990).
16. Baiker, A., Kilo, M., Maciejewski, M., Menzi, S., and Wokaun, A., "Proceedings of the 10th International Congress on Catalysis, Budapest, 1992" (L. Guczi, F. Solymosi, and P. Tetenyi, Eds.), p. 1257. Akadémiai Kiadó, Budapest, 1993.
17. Weigel, J., Koeppel, R. A., Baiker, A., and Wokaun, A., *Langmuir* **12**, 5319 (1996).
18. Fisher, I. A., and Bell, A. T., *J. Catal.* **172**, 222 (1997).
19. Hicks, R. F., Kellner, C. S., Savatsky, B. J., Hecker, W. C., and Bell, A. T., *J. Catal.* **71**, 216 (1981).
20. Fisher, I. A., and Bell, A. T., *J. Catal.* **162**, 54 (1996).
21. Pritchard, J., Catterick, T., and Gupta, R. K., *Surf. Sci.* **53**, 1 (1975).
22. Monti, D. M., Cant, N. W., Trimm, D. L., and Wainwright, M. S., *J. Catal.* **100**, 17 (1986).
23. Millar, G. J., Rochester, C. H., and Waugh, K. C., *J. Chem. Soc. Faraday Trans.* **87**, 2795 (1991).
24. Clarke, D. B., Lee, D. K., Sandoval, M. J., and Bell, A. T., *J. Catal.* **150**, 81 (1994).
25. Wovchko, E. A., Camp, J. C., Glass, J. A., and Yates, J. T., *Langmuir* **11**, 2592 (1995).
26. Millar, G. J., Rochester, C. H., Howe, C., and Waugh, K. C., *J. Chem. Soc. Faraday Trans.* **87**, 1467 (1991).
27. Edwards, J. F., and Schrader, G. L., *J. Phys. Chem.* **88**, 5620 (1984).
28. Millar, G. J., Rochester, C. H., and Waugh, K. C., *Chem. Soc. Faraday Trans.* **87**, 1491 (1991).
29. Fisher, I. A., and Bell, A. T., unpublished results.
30. Millar, G. J., Rochester, C. H., and Waugh, K. C., *Catal. Lett.* **14**, 289 (1992).
31. Kondo, J., Abe, H., Sakata, Y., Maruya, K., Domen, K., and Onishi, T., *J. Chem. Soc. Faraday Trans. 1* **84**, 511 (1988).
32. Guglielminotti, E., *Langmuir* **6**, 1455 (1990).
33. Tret'yakov, N. E., Pozdnyakov, D. V., Oranskaya, O. M., and Filimonov, V. N., *Russ. J. Phys. Chem.* **44**, 596 (1970).
34. Bianchi, D., Chafik, T., Khalfallah, M., and Teichner, S. J., *Appl. Catal. A* **112**, 57 (1994).
35. Bianchi, D., Chafik, T., Khalfallah, M., and Teichner, S. J., *Appl. Catal. A* **112**, 219 (1994).
36. Chafik, T., Bianchi, D., and Teichner, S. J., *Topics Catal.* **2**, 103 (1995).
37. He, M. Y., and Ekerdt, J. G., *J. Catal.* **87**, 381 (1984).
38. Hertl, W., *Langmuir* **5**, 96 (1989).
39. Morterra, C., and Orio, L., *Mater. Chem. Phys.* **24**, 247 (1990).
40. He, M. Y., and Ekerdt, J. G., *J. Catal.* **90**, 17 (1984).
41. Bianchi, D., Chafik, T., Khalfallah, M., and Teichner, S. J., *Appl. Catal. A* **123**, 89 (1995).
42. Bianchi, D., Chafik, T., Khalfallah, M., and Teichner, S. J., *Appl. Catal. A* **105**, 223 (1993).
43. Stuve, E. M., Madix, R. J., and Sexton, B. A., *Surf. Sci.* **119**, 279 (1982).
44. Lavalley, J. C., Lamotte, J., Busca, G., and Lorrenzelli, V., *J. Chem. Soc., Chem. Commun.* 1006 (1985).
45. Onishi, T., Abe, H., Maruya, K., and Domen, K., *J. Chem. Soc., Chem. Commun.* 103 (1986).
46. Idriss, H., Hindermann, J. P., Kieffer, R., Kiennemann, A., Vallet, A., Chauvin, C., Lavalley, J. C., and Chaumette, P., *J. Mol. Catal.* **42**, 205 (1987).
47. Jackson, N. B., and Ekerdt, J. G., *J. Catal.* **101**, 90 (1986).
48. Fakley, M. E., Jennings, J. R., and Spencer, M. S., *J. Catal.* **118**, 483 (1989).
49. Bianchi, D., Gass, J. L., Khalfallah, M., and Teichner, S. J., *Appl. Catal. A* **101**, 297 (1993).
50. Sandoval, M. J., and Bell, A. T., *J. Catal.* **144**, 227 (1993).
51. Burch, R., Golunski, S. E., and Spencer, M. S., *J. Chem. Soc. Faraday Trans.* **86**, 2683 (1990).
52. Sellmer, G., Prins, R., and Kruse, N., *Catal. Lett.* **47**, 83 (1997).
53. Fujita, S., Usui, M., Ito, H., and Takezawa, N., *J. Catal.* **157**, 403 (1995).